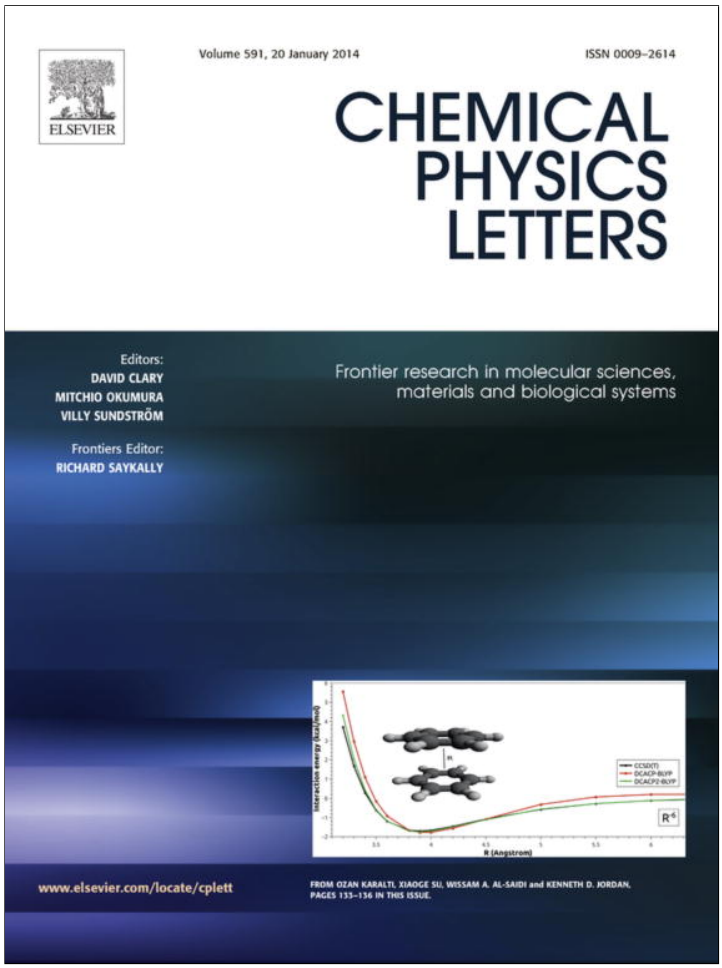

Chemical Physics Letters 591 (2014) 161–165

Contents lists available at ScienceDirect

Chemical Physics Letters

journal homepage: www.elsevier.com/locate/cplett

Exploiting the ion-exchange ability of titanate nanotubes in a model water softening process

Dániel Madarász [a], Imre Szenti [a], András Sápi [a], János Halász [a], Ákos Kukovecz [a,b], Zoltán Kónya [a,c,*]

[a] Department of Applied and Environmental Chemistry, University of Szeged, Rerrich Béla tér 1, Szeged H-6720, Hungary
[b] MTA-SZTE 'Lendület' Porous Nanocomposites Research Group, Rerrich Béla tér 1, Szeged H-6720, Hungary
[c] MTA-SZTE Reaction Kinetics and Surface Chemistry Research Group, Rerrich Béla tér 1, Szeged H-6720, Hungary

ARTICLE INFO

Article history:
Received 19 September 2013
In final form 8 November 2013
Available online 21 November 2013

ABSTRACT

Titanate nanotubes were utilized in Ca^{2+} and Mg^{2+} removal in a continuous ion-exchange unit. Three consecutive water softening–regeneration cycles were performed. The highest measured value of the total ion-exchange capacity was 1.2 mmol g^{-1} which decreased to 0.66 mmol g^{-1} in the third cycle. The capacity loss was due to the irreversible binding of Ca^{2+} ions to very strong adsorption sites, while the Mg^{2+}/Na^{+} exchange was reversible. A relatively fast initial adsorption step and a subsequent slower concentration decrease were the two processes that governed the kinetics of the ion exchange reaction.

1. Introduction

Removal of unwanted ions from drinking, industrial, waste and other types of water is an integral part of technology planning and design. It is also the main topic for several studies focused on 'green' processing. Large bodies of surface and groundwaters polluted with heavy ions and radioactive materials are still in need of remediation and purification worldwide. For instance, the 2011 earthquake-induced nuclear disaster in Fukushima, Japan resulted in millions of tons of seawater getting polluted with radioactive materials such as ^{137}Cs which has spread all over the world since then.

Softened water is a basic requirement for several technological and domestic applications. Ca^{2+} and Mg^{2+} ions cause water hardness and are directly responsible for scale and other unwanted precipitate formation as well as for the deterioration of the efficiency of detergents (e.g. soap). Scale can plug pipelines, reduce the heat transfer efficiency in cooling or heating applications and may lead to furnace or boiler blasting. Several types of water softening processes such as ion exchange, evaporation, precipitation, ultrafiltration, nanofiltration and electrodeionization are used today [1–4]. Among them, ion exchange is popular due to its ease of operation and high 'hard' ion removal efficiency [3].

Materials in the nanometer scale are extensively researched in ion removal and adsorbent applications because of their large specific surface area and other potentially beneficial properties such as special morphologies and controllable size distributions. Carbon nanotubes have great potential in water treatment and environmental protection [5–9] because of the many possibilities they offer for surface modification [10–14]. This resulted in the synthesis of carbon nanotube based specific adsorbents and ion exchangers capable of removing unwanted ions from water. Zero dimensional metal-oxide nanoparticles provide superior adsorption kinetics for the removal of metal ions from aqueous solutions [15,16]. By using magnetic iron oxide nanoparticles, the effective remediation can even be combined with a straightforward solid–liquid separation process [17,18].

Titanate nanotubes (TiONTs) are also promising ion exchanger material candidates. These one-dimensional nanomaterials have a 'rolled-up' layered structure [19]. The layers are made of TiO_6 octahedrons resulting in a negatively charged nanotube skeleton in which the charge is compensated by cations located in ion exchange positions on the nanotube surface, at the tips and in between the layers [20]. These cations are mobile which endows TiONTs with cation exchange properties resulting in a new type of ionexchanger material with considerable application potential [21,22]. Expecting a stoichiometric reaction ($Na_2Ti_3O_7 + M^{2+} \leftrightarrow MTi_3O_7 + 2Na^{+}$), the theoretical maximum ion-exchange capacity of TiONTs is approximately 2.9 mmol g^{-1} for bivalent cations (taking into account the ~10 w% water content of TiONTs).

In the present study, our aim was to exploit the ion exchange properties of titanate nanotubes in a model water softening process. Hard water containing Ca^{2+} and Mg^{2+} ions was softened in a continuous operation fixed-bed column. Sodium chloride based regeneration was applied between softening cycles. The concentration of 'hard' ions was monitored by classical analytical methods and thus the ion exchange capacity was determined. An independent ion adsorption kinetic study was performed to facilitate the understanding of the behavior of titanate nanotubes in the ion exchange process.

* Corresponding author at: Department of Applied and Environmental Chemistry, University of Szeged, Rerrich Béla tér 1, Szeged H-6720, Hungary.
E-mail address: konya@chem.u-szeged.hu (Z. Kónya).

0009-2614/$ - see front matter © 2013 Elsevier B.V. All rights reserved.
http://dx.doi.org/10.1016/j.cplett.2013.11.021

2. Experimental

2.1. Synthesis and characterization

Titanate nanotubes were synthesized by a simple alkali hydrothermal method as described previously [23–25]. Briefly, the preparation was performed by the alkaline recrystallization of anatase TiO_2. 70 g of TiO_2 (Sigma–Aldrich) was mixed with 1 L 10 M aqueous NaOH (Molar) solution under intensive stirring until a white suspension was obtained, then the suspension was aged in a closed, cylindrical, PTFE-lined autoclave at 125 °C for 48 h. The product was washed with 0.1 M HCl (Molar) solution and deionized water to reach neutral pH. The slurry was filtered and dried in air at 60 °C. The obtained material was characterized by transmission electron microscopy (TEM, Philips CM10, 100 kV) and X-ray diffractometry (XRD, RigakuMiniflex2, CuK_α). The specific surface area was determined from nitrogen adsorption measurements performed at 77 K in a Quantachrome Nova 3000e instrument and analyzed by the BET method. Artificial hard water was made of analytical grade $Mg(NO_3)_2 * 6H_2O$ (Reanal) and $CaCl_2 * 2H_2O$ (Reanal).

The elemental composition of the titanate nanotubes was analyzed by energy dispersive X-ray spectroscopy (Röntec Quantax^2 EDS) built into a Hitachi S-4700 Type II cold field emission scanning electron microscope. Samples were drop-casted from alcoholic suspension onto silicon wafers and measured at 10 kV accelerating voltage without any additional coating.

2.2. Ion exchange experiments

TiONT-based water softening experiments were performed in a continuous flow fixed bed apparatus (Figure 2A) at room temperature. The ion exchange bed contained 12 g TiONTs. In order to achieve a well-defined starting condition, the TiONT bed was treated with 4 L of 2.56 M NaCl solution and rinsed with 1 L 0.05 M NaCl solution before the water softening process. In the actual experiment, artificial hard water with a total hardness of ~60 GH° (0.01 M) and a Ca^{2+}:Mg^{2+} ion ratio of 1:1 was pumped through the reactor with a feeding rate of 1.6 L h^{-1} until chemical analysis indicated that the column was exhausted. The TiONT bed was then regenerated by repeating the NaCl solution treatment described above. Three softening–regeneration cycles were performed. For comparison, the water softening process was also carried out on a commercial DOWEX-50 W ion-exchange resin as a reference.

The hardness of the water at the column outlet was monitored by chelatometric titration in every 20 min. Firstly, 2 mL 10w% aqueous NaOH solution was added to 100 mL of water sample to mask the Mg^{2+} ions. The Ca^{2+} ion concentration was then determined using murexide (Reanal) indicator and EDTA (Reanal) solution. After reaching the equivalence point, 3 mL of 20 w% HCl solution and 6 mL 25 w% of NH_4OH solution were added to the titrated sample and the solution was titrated further using eriochrome black T (Reanal) indicator to measure the Mg^{2+} ion concentration.

In the ion adsorption kinetic investigation, 3–3 g of NaCl solution pretreated TiONT was suspended in 600 mL of ~60 GH° hard water as well as in 600–600 mL ~50 GH° (0.009 M) Ca^{2+} and Mg^{2+} solution under vigorous stirring. The mixtures were sampled at regular intervals during the course of the 164 h long experiments. The solutions was separated from the TiONTs by centrifugation and the samples were analyzed for Ca^{2+} and Mg^{2+} by chelatometry as described above (the centrifuged titanate nanotubes were reintroduced into the mixture).

3. Results and discussion

3.1. Ion exchange capacity

TEM images of the initial TiO_2 (anatase) material show the presence of isotropic nanoparticles with a diameter of 50–130 nm (Figure 1A). In contrast, the as-synthesized titanate nanotubes (TiONTs) are open-ended hollow tubular objects measuring 100–150 nm in length and 6–10 nm in diameter (Figure 1B). A typical titanate nanotube has 4 walls and approximately 0.73 nm interlayer spacing.

The synthesized white, powder-like material was identified as sodium–hydrogen–trititanate ($Na_xH_{2-x}Ti_3O_7$) by XRD (Figure 1C). Weak and broadened reflections indicate that the material is of lower crystallinity compared to the initial anatase material. Peaks marked as 'A' and 'T' are characteristic of the anatase and trititanate structures, respectively. The specific surface area of titanate nanotubes is ~185 m^2 g^{-1} because of their tubular morphology and readily accessible inner channel surface.

The schematics of the apparatus used in the actual water softening experiments is presented in Figure 2A, whereas Figure 2B depicts the breakthrough curves of the first cycle of the TiONT based water softening process. The total hardness (Ca^{2+} + Mg^{2+} ions) and the individual Ca^{2+} and Mg^{2+} ion concentrations measured at the column outlet are presented. The column was totally exhausted after pumping 6.3 L hard water through it as described above. The ion exchange capacity calculated from the breakthrough curve is 1.2 mmol g^{-1}, which is approximately 41% of the theoretical maximum TiONT ion exchange capacity. It is interesting to note that while the Mg^{2+} ion concentration in the effluent increased rapidly at the beginning of the process, the Ca^{2+} ion concentration was much slower to converge to its final value. The Mg^{2+} breakthrough curve features a characteristic local maximum at about 25% of total time on stream and the magnesium concentration in the effluent at this maximum is actually higher than in the feed. This apparent contradiction can be explained by assuming that Mg^{2+} ions initially captured by the TiONTs are eluted by the more preferred Ca^{2+} ions at this stage (Nagy et al., 1998). The reason behind this is the ion adsorption competition of the different ions with different effective nuclear charges, adherent hydrospheres and hydration energies. The ion radii of hydrated Ca^{2+} and Mg^{2+} ions are 0.30 nm and 0.34 nm, respectively. The smaller ion radius facilitates Ca^{2+} migration into the layers of the trititanate structure. Moreover, the hydrated Ca^{2+} and Mg^{2+} ions must strip their hydrate shells in order to occupy TiONT ion exchange positions. Therefore, hydration energy affects selectivity: the lower the hydration energy, the higher the ion exchange affinity [26]. The hydration energy of Ca^{2+} and Mg^{2+} is 1592.4 kJ mol^{-1} and 1922.1 kJ mol^{-1}, respectively. In summary, smaller ion radius and lower hydration energy of Ca^{2+} result in the long-term preferential adsorption of Ca^{2+} ions against Mg^{2+} on titanate nanotubes.

The total ion exchange capacity of the TiONT column decreased gradually during the first three consecutive softening–regeneration cycles (Figure 3A). The ion exchange capacity dropped from 1.2 mmol g^{-1} to 0.89 mmol g^{-1} in the second cycle and then further to 0.66 mmol g^{-1} in the third one, corresponding to 41%, 30% and 22% of the theoretical maximum ion exchange capacity, respectively. The ion exchange capacities are smaller than that of the reference DOWEX-50W resin (2.33 mmol g^{-1}). The detailed analysis of the individual ion exchange curves depicted in Figure 3B and C revealed that the loss of total ion exchange capacity was almost exclusively due to the loss of Ca^{2+} sorption capacity. The Ca^{2+} breakthrough curves have shifted systematically to the left with each cycle. The Ca^{2+} sorption capacity of the TiONT bed dropped from 0.92 mmol g^{-1} to 0.64 mmol g^{-1} and then to 0.45 mmol g^{-1}.

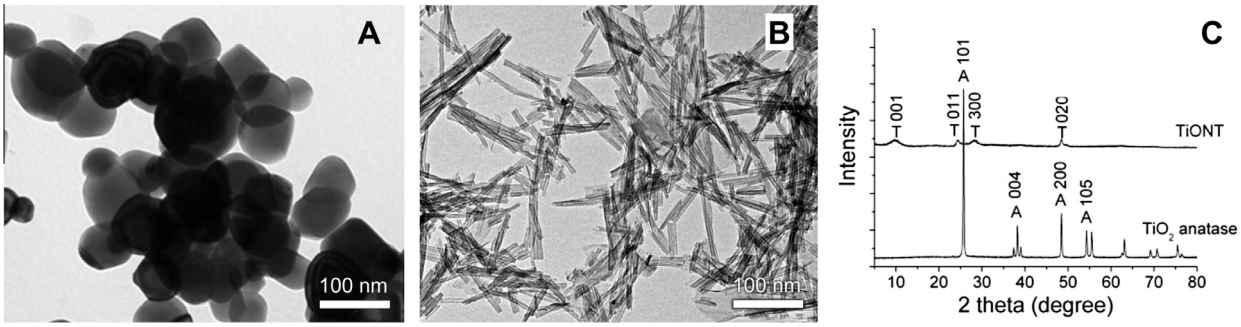

Figure 1. Typical TEM images of the initial titanium-dioxide (anatase) (A), as-synthesized titanate nanotubes (B) and the corresponding XRD patterns (C).

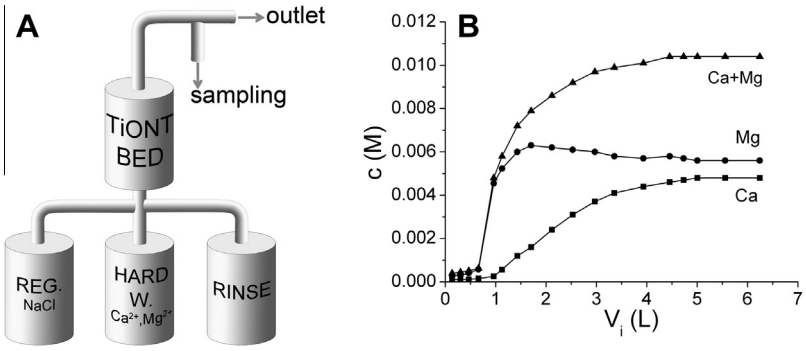

Figure 2. Schematic view of the TiONT-based water softening apparatus (A) and breakthrough curve of the first cycle of the hardness removal process (B).

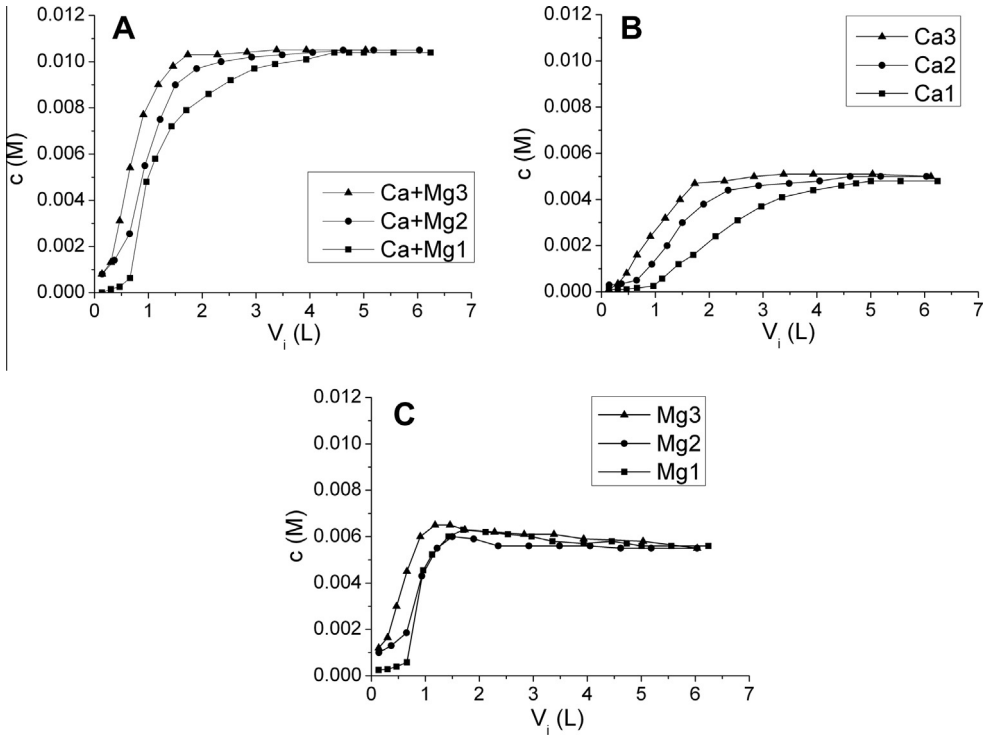

Figure 3. Total hardness (A), Ca^{2+} ion (B) and Mg^{2+} ion (C) concentration breakthrough curves measured in three consecutive softening–regeneration cycles. The cycle number is indicated in the curve tag.

On the other hand, Mg^{2+} ion breakthrough curves have suffered significantly less changes during the repetitions, corresponding to Mg^{2+} sorption capacities of 0.28 mmol g^{-1}, 0.26 mmol g^{-1} and 0.21 mmol g^{-1} in the three consecutive softening–regeneration cycles, respectively. This indicates that the Mg^{2+} ion capacity of a TiONT bed is almost constant but the Ca^{2+} ion bonding ability of the TiONT-based ion exchanger deteriorates with time under the used softening–regeneration parameters.

Table 1
EDS derived alkaline element content of TiONT after subsequent softening and regeneration cycles.

	A (at.%)/Ti (at.%) * 100					
	Softening cycles			Regeneration cycles		
	1	2	3	1	2	3
Sodium	7.4	6.1	8.0	23.7	24.1	24.6
Magnesium	4.8	5.3	5.6	–	–	4.3
Calcium	9.4	11.3	12.3	4.5	7.7	7.3

The energy dispersive X-ray analysis (EDS) of the TiONT water softening cartridge after the first exhaustion revealed the presence of adsorbed magnesium and calcium as well as sodium, titanium and oxygen which are attributed to the pristine TiONT material (the sign of the Si is attributed to the sample holder) (Table 1, Figure 4A). No significant change in the crystal structure of titanate nanotubes could be observed by XRD (not shown here). The higher amount of calcium compared to magnesium in the sample confirms the stronger Ca^{2+} ion bonding affinity of TiONT. The more favorable adsorption of Ca^{2+} ions in the TiONT-based ion exchange is similar to the behavior of zeotype materials and ion exchange resins in such ion adsorption processes [27–30]. The remnant sodium content of the sample is attributed to Na^{+} ions bonded to inaccessible cation positions found deep within the nanotube walls. After regeneration, the increased sodium content can be attributed to the elution of hard ions and their replacement by Na^{+} (Figure 4B). The EDS profile of the regenerated sample reveals the presence of calcium but the lack of magnesium. This finding agrees well with the observed gradual loss of calcium and preservation of magnesium ion exchange capacity and indicates that calcium is more strongly bonded to the adsorption sites of TiONTs.

3.2. Ion exchange kinetics

The adsorption of both Ca^{2+} and Mg^{2+} on TiONTs was studied as a function of time in order to gain insight into the adsorption kinetics of these ions on anisotropic titanate nanostructures. Adsorption experiments were carried out from the individual solutions of Ca and Mg salts and from the mixture of the hard ions as well. The concentration of the cations was monitored after titanate nanotubes were introduced to the solutions under vigorous stirring. The change of the concentrations during time is nearly identical in every case (Figure 5). Bivalent ion concentration in the artificially hardened water and in the individual hard ion solutions was reduced rapidly after introducing the TiONTs. The 'hard' ion concentration was almost halved in the first 5 h of the ion exchange process. Afterwards, the ion adsorption slowed down. These results correlate well with literature findings. Bavykin and Walsh studied the ion exchange kinetics of the Li^{+}/TiONT system by monitoring the changes in pH after adding LiOH solution into the suspension of protonated TiONT. After introducing the LiOH solution to the suspension the pH reached a maximum value, then dropped quickly again because of the Li^{+}/H^{+} ion exchange. After the rapid initial reaction the ion exchange process slowed down and was completed in a few tens of minutes in the applied reaction environment [21]. Wang et al. also report a rapid initial reaction between Cu^{2+} and TiONT which slowed down and reached equilibrium after a few hours [31].

In the cases of Ca^{2+} and Mg^{2+} the alkaline ion concentrations of the solutions decreased rapidly first and much slower afterwards (Figure 5A). In the first 20 min the Ca^{2+} ion concentration in the solution was decreasing with a rate of 2.31 mmol g^{-1} h^{-1}, while the decreasing rate of Mg^{2+} was smaller: 1.79 mmol g^{-1} h^{-1} (Table 2) which rates degreased further. After 48 h of TiONT exposure the ion concentration in the Ca^{2+} solution became almost constant (~0.001 mmol g^{-1} h^{-1}) and constant in the Mg^{2+} solution. In case of artificial hard water (mixture of Ca^{2+} and Mg^{2+} solutions with ~60 GH° and 1:1 M ratio of hard ions) the higher affinity of TiONT to Ca^{2+} against Mg^{2+} was also observed (Figure 5B). The adsorption speed of Ca^{2+} was much higher than that of Mg^{2+}, 1.83 mmol g^{-1} h^{-1} and 0.79 mmol g^{-1} h^{-1}, respectively, in the first 20 min. Afterward, these rates were decreased further as well as in case of individual Ca^{2+} and Mg^{2+} solutions (Table 2). In addition, the total ion exchange capacity was calculated to 1.73 mmol g^{-1}, which splits to 1.02 mmol g^{-1} Ca^{2+} and 0.71 mmol g^{-1} Mg^{2+} ion bonding capacities. We suggest that the first rapid ion exchange step is related to ion binding to easily accessible sites located at the tips as well as the inner and outer cylindrical tube surfaces of the titanate nanotubes (Figure 6). On the other hand, the subsequent slow ion exchange process originates from ion binding to less accessible adsorption sites within the wall-forming layers. The high activation energy of ion migration from and into the interlayer spacing is responsible for the slow ion exchange process.

These data confirm that the adsorption of calcium is thermodynamically preferred over magnesium because of its smaller ion radius and lower hydration energy. Therefore, Ca^{2+} gradually replaces the initially adsorbed magnesium ions which are released into the effluent. The local Mg^{2+} concentration maximum observed in Figure 2B is due to the temporal overlapping of this magnesium release from the TiONTs and the default magnesium concentration of the feed at the column outlet.

The amount of 'easily accessible sites' of TiONTs was calculated considering a typical TiONT (125 nm length, 8 nm outer diameter, 4 layers with 0.73 nm interlayer distance, hypothesized as 4 coaxial cylindrical tubes for simplification) taking into account only the external surfaces of outer walls, the inner surfaces of the inner

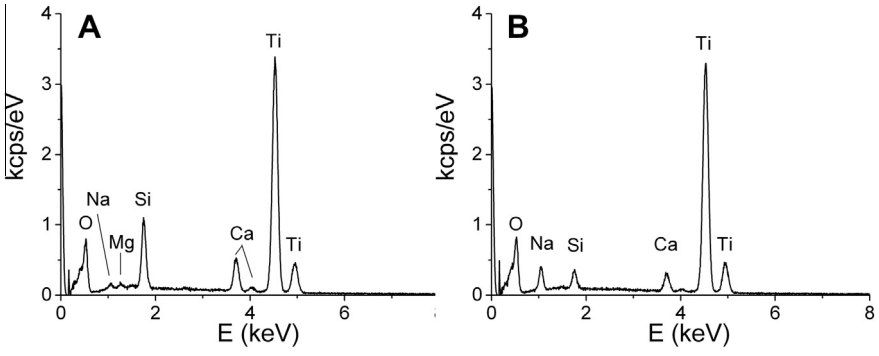

Figure 4. EDS spectra of TiONT after the first softening (A) and subsequent regeneration (B) cycle.

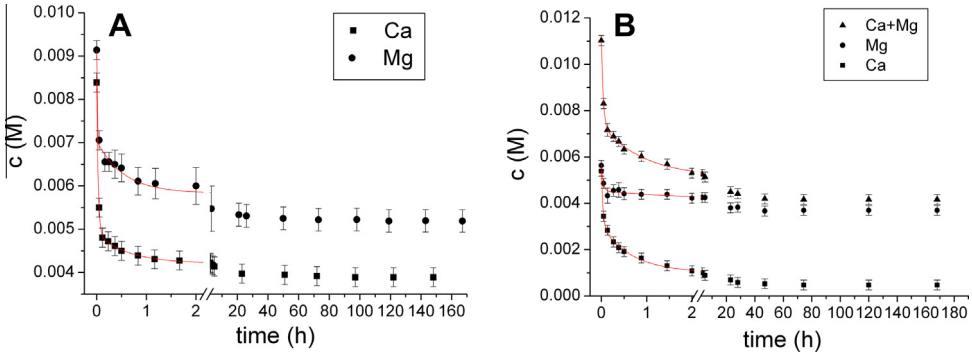

Figure 5. Kinetics of the Ca^{2+} and Mg^{2+} ion adsorption process on titanate nanotubes from Ca and Mg solution (A) and from Ca + Mg solution (B) – lines are drawn to guide the eye.

Table 2
Speed of the ion exchange process on TiONTs as a function of time.

Period	Speed of ion exchange (mmol g^{-1} h^{-1})				
	Individually		Mixed		
	Ca	Mg	Ca	Mg	Ca + Mg
0–20 min	2.313	1.794	1.831	0.792	2.623
20–120 min	0.133	0.153	0.129	0.110	0.239
2–48 h	0.008	0	0.005	0.002	0.007
48–168 h	0.001	0	0.001	0	0.001

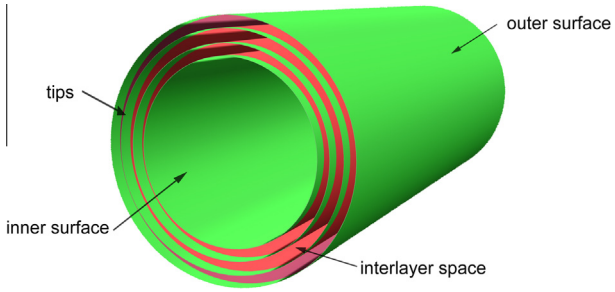

Figure 6. Simplified model of TiONT, location of easy accessible sites (green) and interlayer space (red). (For interpretation of the references to color in this figure legend, the reader is referred to the web version of this article.)

layers and the tips. The calculated total amount of these positions is ~0.75 mmol g^{-1} which correlates well with the kinetic measurements, where 0.82 mmol g^{-1} ion was found to be bonded in the very first rapid reaction period between the titanate nanotubes and 'hard' ions.

4. Conclusion

Titanate nanotubes (TiONTs) were successfully synthesized and used in a continuous flow fixed bed ion exchange column for the removal of 'hard' alkali earth metal ions from aqueous solutions. High amounts of Ca^{2+} and Mg^{2+} ions can be removed by TiONTs due to their relatively high specific surface area, accessible hollow interior and negatively charged, ion-exchange capable framework. We have demonstrated that there are at least two types of ion exchange sites in TiONTs distinguishable on the basis of their differing adsorption kinetics. Cations are rapidly adsorbed on the surfaces and tips of nanotubes, whereas ion exchange is significantly slower at sites located in the interlayer spacing of the one dimensional nanomaterial framework. The limited success in the recovery of calcium ions from the TiONT bed under the applied experimental parameters can be attributed to the strong interaction between Ca^{2+} ions and calcium-selective adsorption sites. Although more detailed studies are necessary to exactly identify these sites in the nanotube framework, it is clear that this irreversible bonding could be exploited in e.g. radioactive (or any other unwanted) ion removal and safe storage in the future.

Acknowledgements

The financial support of the TÁMOP-4.2.2.A-11/1/KONV-2012-0047 and OTKA K 83889 projects is acknowledged.

References

[1] B. Bruggen, C. Vandecastelee, Environ. Pollut. 122 (2003) 435.
[2] J.H. Kweon, D.F. Lawler, Drinking Water Eng. Sci. 38 (2004) 4164.
[3] H.J. Lee, M.K. Hong, S.H. Moon, Desalination 284 (2012) 221.
[4] G.P. Rao, C. Lu, F. Su, Sep. Purif. Technol. 58 (2007) 224.
[5] C. Chen, X. Wang, Ind. Eng. Chem. Res. 45 (2006) 9144.
[6] Y.H. Li, S. Wang, Z. Luan, J. Ding, C. Xu, D. Wu, Carbon 41 (2003) 1057.
[7] X.L. Tan, D. Xu, C.L. Chen, X.K. Wang, W.P. Hu, Radiochim. Acta 96 (2008) 23.
[8] T. Wang, W. Liu, N. Xu, J. Ni, J. Hazard. Mater. 250–251 (2013) 379.
[9] W.L. Yim, Z.F. Lin, Chem. Phys. Lett. 398 (2004) 297.
[10] J. Chen, M.A. Hamon, H. Hu, Y. Chen, A.M. Rao, P.C. Eklund, R.C. Haddon, Science 282 (1998) 95.
[11] T.W. Ebbesen, H. Hiura, M.E. Bisher, M.M.J. Treacy, J.L. Shreeve-Keyer, R.C. Haushalter, Adv. Mater. 8 (1996) 155.
[12] M.A. Hamon et al., Adv. Mater. 11 (1999) 834.
[13] E.T. Mickelson, C.B. Huffman, A.G. Rinzler, R.E. Smalley, R.H. Hauge, J.L. Margrave, Chem. Phys. Lett. 296 (1998) 188.
[14] F. Pompeo, D.E. Resasco, Nano Lett. 2 (2002) 369.
[15] J.S. Hu, L.S. Zhong, W.G. Song, L.J. Wan, Adv. Mater. 20 (2008) 2977.
[16] L.S. Zhong, J.S. Hu, H.P. Liang, A.M. Cao, W.G. Song, L.J. Wan, Adv. Mater. 18 (2006) 2426.
[17] X. Liu, Q. Hu, Z. Fang, X. Zhang, B. Zhang, Langmuir 25 (2009) 3.
[18] P. Saravanan, V.T.P. Vinod, B. Shreedhar, R.B. Sashidhar, Mater. Sci. Eng. C 32 (2012) 581.
[19] T. Kasuga, M. Hiramatsu, A. Hoson, T. Sekino, K.K. Niihara, Langmuir 14 (1998) 3160.
[20] D.V. Bavykin, V.N. Parmon, A.A. Lapkin, F.C. Walsh, J. Mater. Chem. 14 (2004) 3370.
[21] D.V. Bavykin, F.C. Walsh, J. Phys. Chem. C 111 (2007) 14644.
[22] S.S. Lium, C.K. Lee, H.C. Chen, C.C. Wang, L.C. Juang, Chem. Eng. J. 147 (2009) 188.
[23] E. Horváth, Á. Kukovecz, Z. Kónya, I. Kiricsi, Chem. Mater. 19 (2007) 927.
[24] Á. Kukovecz, M. Hodos, E. Horváth, G. Radnóczi, Z. Kónya, I. Kiricsi, J. Phys. Chem. B 109 (2005) 17781.
[25] (a) M.C. Wu et al., ACS Nano 5 (2010) 5025;
(b) M.C. Wu et al., Nano Res. 4 (2011) 360;
(c) M.C. Wu et al., J. Nanosci. Nanotechnol. 12 (2012) 1421.
[26] W. Liu, T. Wang, A.G.L. Borthwick, Y. Wang, X. Yin, X. Li, Y. Ni, Sci. Total Environ. 456–457 (2013) 171.
[27] J.B. Nagy, P. Bodart, I. Hannus, I. Kiricsi, Synthesis, Characterization and Use of Zeolitic Microporous Materials, DecaGen Ltd., Szeged, 1998.
[28] G. Rytwo, A. Banin, S. Nir, Clays Clay Miner. 44 (1996) 276.
[29] S.A.I. Barri, L.V.C. Rees, J. Chromatogr. 201 (1980) 21.
[30] Z. Yua, T. Qi, J. Qu, L. Wang, J. Chu, J. Hazard. Mater. 167 (2009) 406.
[31] X. Wang, C. Chen, W. Hu, A. Ding, D. Xu, X. Zhou, Environ. Sci. Technol. 39 (2005) 2856.